Energy Metrics to Evaluate the Energy Use and Performance of Water Main Assets

Saeed Hashemi[1], Yves R. Filion[2], Vanessa L. Speight[3]

Abstract: Managing aging infrastructure has become one of the greatest challenges for water utilities, particularly when faced with selecting the most critical pipes for rehabilitation from amongst the thousands of candidates. The aim of this paper is to present a set of novel yet practical energy metrics that quantify energy interactions at the spatial resolution of individual water mains to help utilities identify pipes for rehabilitation. The metrics are demonstrated using a benchmark system and two large, complex systems. The results show that the majority of pipes have a good energy performance but that an important minority of outlier pipes have a low energy efficiency and high energy losses due to friction and leakage. Pumping and tank operations tend to drive energy efficiency and energy losses in pipes close to water sources while diurnal variation in demand drives energy performance of mains located far away from water sources. The new metrics of energy lost to friction and energy lost to leakage can provide information on energy performance in a pipe than is complementary to the traditional measures of unit headloss and leakage flow.

Keywords: Energy efficiency, energy metrics, friction loss, leakage loss, pipe rehabilitation, water distribution systems.

[1] Saeed Hashemi, Graduate Student, Queen's University, Kingston, Ontario, Canada, K7L 3N6 (e-mail: s.hashemi@queensu.ca).
[2] Yves R. Filion, Associate Professor, Queen's University, Kingston, Ontario, Canada, K7L 3N6 (e-mail: yves.filion@civil.queensu.ca).
[3] Vanessa Speight, Senior Research Fellow, University of Sheffield, Sheffield, UK, S1 3JD, (e-mail: v.speight@sheffield.ac.uk).

Introduction

Water distribution systems play host to a multitude of energy interactions on an hourly and daily basis. Pumps and reservoirs supply mechanical energy to the system, while water demand, pipe leaks, and frictional headloss provide output pathways for energy to leave the system, either in the form of work or heat. As water main assets in a system age and deteriorate, they become less energy efficient, with more energy leaving the system via unwanted pipe leaks and through frictional headloss (Fontana et al., 2012; Kleiner and Rajani, 2001). The challenge in managing a large, aging water distribution system is to prioritize interventions so that investment returns the largest gain in system performance (Alvisi and Franchini, 2009 and 2006, Dandy and Engelhardt, 2001).

Energy has long been used as a key concept to understand the performance of engineering systems (Pelli and Hitz 2000; Lambert et al., 1999). Energy use as a modeling concept is germane to understanding the energy performance of water main assets in distribution systems because power and energy in water distribution systems depend on pressure and flow – two quantities that are monitored continuously by water utilities (Dziedzic and Karney, 2015; AWWA, 2009; Boulos et al., 2006). While most municipalities extensively monitor their systems, few have a firm understanding of the energy efficiency of their systems. Even fewer municipalities have the capability to use pressure and flow data to understand the impact of infrastructure upgrades and operational changes on the energy efficiency of their systems (Engelhardt et al., 2000; Roshani and Filion, 2013; Hashemi et al., 2012).

To date, previous research has been focused on characterizing the system-wide energy dynamics in distribution systems. Colombo and Karney (2002) showed that diurnal demand/pressures can affect the manner in which fissures and cracks in pipes conduct leakage.

Results demonstrated that the more distant the leakage sources are from the water sources, the higher is the energy lost from leakage and friction. While, the presence of storage was shown to have a negligible effect on leakage energy, the location of the tanks did influence the leakage level and pumping energy (Colombo and Karney 2005). The research underscored the important role of water mains, and their proximity to pumps and tanks, on the energy balance of a system.

Energy metrics developed thus far have focused on the system-wide energy performance of systems. Pelli and Hitz (2000) developed energy indicators to relate system-wide energy efficiency to pump efficiency and reservoir location, without considering leakage impacts. Cabrera et al. (2010) presented a set of metrics to characterize the system-wide energy performance that includes losses to friction, leakage, and overpressure. These energy metrics provide a useful set of tools to help water utility managers better understand how far their systems are from an ideal energy-efficient state but fall short of being able to identify individual pipes that are problematic. Building upon their earlier work, Cabrera et al. (2014b) presented additional metrics to assess the energy efficiency of a pressurized system and procedures to prioritize interventions on a system-wide basis. Dziedzic and Karney (2014) examined the energy dynamics of groups of pipes and pumps in the Toronto distribution system. While these researchers also solved the energy balance to examine the frictional losses in individual pipes of the Toronto system, they did not examine the efficiency, leakage, and other energy characteristics of these pipes. The current paper extends this research direction by considering energy transformations that take place in the individual pipes of a distribution system.

The aim of this paper is to present a set of novel energy metrics that quantify energy interactions in a distribution system at the spatial resolution of individual water mains. These pipe-level metrics can be applied to: 1) characterize the energy performance in water mains in an

unimproved state to establish a benchmark prior to any rehabilitation work; 2) plan infrastructure upgrades and operational changes in areas that exhibit a low energy efficiency alongside information on cost, water quality, and pipe break history, and; 3) characterize the impact of infrastructure upgrades and operational improvements on the energy performance of water mains in a system. In this paper, the new pipe-level metrics are applied to a large *ensemble* of water mains across three distribution systems to examine how system operation and system improvements impinge on the spatial and temporal patterns of energy performance in drinking water mains.

Energy Use in a Pipe

To develop a set of energy metrics, it is instructive to consider the hydraulic grade line with energy inputs and outputs in a single pipe as indicated in Figure 1. Here, the pipe conveys a flow Q (m^3/s) at an upstream pressure head H_s (m). The pipe delivers a pressure head H_d (m) to a downstream user that imposes a demand Q_d (m^3/s) in the pipe. Users downstream of a pipe impose a demand Q_d (m^3/s) that exceeds the minimum needed water use Q_{min} (m^3/s), which represents the most efficient use of water by the user given best-available water technologies (Vickers 2001). There are a number of reasons for this inefficient water use including household leaks, inefficiencies in appliances, theft of water (AWWA 2009), water waste through inefficient industrial processes (Morales et al. 2011; Friedman et al. 2011), user perception of appropriate water use (Hoekstra and Chapagain 2007), and unnecessary lawn and garden watering (Askew and McGuirk 2004). For the sake of generality, the pipe can have a leak that produces a leakage flow rate of Q_l (m^3/s). The pipe also conveys an additional flow $Q_{ds}=Q-Q_d-Q_l$ (m^3/s) to users further downstream of the pipe. The upstream pressure head H_s (m) supplied to the pipe is greater than the minimum required pressure head H_{min} (m) needed to provide an acceptable

service to the downstream user. The difference between supplied head H_s (m) and pressure head delivered H_d (m) is made up of local losses H_{local} (m) (e.g., valves, in-line turbines, blockages) and the combined frictional head loss due to demand Q_d (m^3/s), leakage Q_l (m^3/s), and the additional flow Q_{ds} (m^3/s) to provide water service to downstream users. The pressure head delivered to downstream users H_d (m) is made up of the minimum pressure head required, H_{min} (m), and surplus head, H_{surplus} (m).

The energy components indicated in Figure 1 are defined in Table 1 and described below.

$$E_{\text{supplied}} = E_{\text{delivered}} + E_{\text{ds}} + E_{\text{leak}} + E_{\text{friction}} + E_{\text{local}} \quad \text{(Joules)} \tag{1}$$

where E_{supplied} = energy supplied to the upstream end of the pipe (Joules); $E_{\text{delivered}}$ = energy delivered to the user (in Joules) to satisfy demand Q_d (m^3/s) at pressure head H_d (m); E_{ds} = energy that flows out of the pipe to meet downstream user demands (Joules); E_{leak} = leak energy (Joules); E_{local} = local energy losses (Joules). The term α is equal to 1.85 in the Hazen-Williams friction loss model and α = 2 in the Darcy-Weisbach model; K = pipe resistance and Δt = the hydraulic time step (3,600 seconds or 1 hour) used in the 24-hour diurnal simulation.

Methods

Metrics to Evaluate Energy Performance at the Pipe Level

Five metrics have been developed to characterize the gross and net energy efficiencies, energy needed by user, energy lost to friction, and energy lost to leakage in the pipes of a water distribution network.

Gross and Net Efficiencies: The gross energy efficiency (*GEE*) in Equation 2 compares the energy delivered to the users serviced by a pipe to the energy supplied to that pipe. The theoretical maximum value for *GEE* is 100 percent, which means that all the energy supplied to the pipe is delivered to its user, even though this is impossible to achieve in practice. The

theoretical minimum value for *GEE* is 0 percent, which means that none of the energy supplied to the pipe is delivered to its users, as all the energy is lost along the pipe.

$$GEE = \left(\frac{E_{\text{delivered}}}{E_{\text{supplied}}} \right) \cdot 100\% \tag{2}$$

The net energy efficiency (*NEE*) in Equation 3 compares the energy delivered to users serviced by a pipe to the net energy in that pipe. Here, net energy is defined as the energy supplied to the pipe minus the energy supplied to users located downstream of the pipe and not directly serviced by the pipe. The maximum value of *NEE* is 100 percent, where all the energy supplied (exclusively to the pipe) is delivered to its users. The theoretical minimum value is 0 percent, where none of the energy supplied to the pipe is delivered to its users.

$$NEE = \left(\frac{E_{\text{delivered}}}{E_{\text{supplied}} - E_{\text{ds}}} \right) \cdot 100\% \tag{3}$$

Energy Needed by User: The energy needed by the users (*ENU*) at a node in Equation 4 compares the energy delivered to the users serviced by a pipe against the minimum energy needed by those users. A value of *ENU* below 100 percent indicates that there is an insufficient level of energy to meet the service expectations of the users (either in the form of flow, pressure head, or both), and a value of 100 percent means that energy delivered to the users is equal to the minimum energy needed to meet their service expectations. Values of *ENU* above 100 percent denote a surplus energy over and above the level needed.

$$ENU = \left(\frac{E_{\text{delivered}}}{E_{\text{need}}} \right) \cdot 100\% \tag{4}$$

The minimum mechanical energy in the water needed to meet the minimum needs of the downstream user in Equation 4 is calculated by integrating the minimum needed power by a

130 defined period of use Δt

$$E_{need} = \gamma Q_{min} H_{min} \Delta t \qquad \text{(Joules)} \tag{5}$$

131 where γ = unit weight of water (approximately 9,810 N/m^3 at 18^{o}C); Q_{min} = minimum water
132 use needed by users (m^3/s); H_{min} = minimum pressure head required to deliver acceptable water
133 service to users (m); Δt= time step over which minimum needed power is integrated (seconds).
134 (Note that integration can be used to calculate minimum energy needed over a continuous diurnal
135 demand period.). Determining the minimum water use (Q_{min}) is difficult because minimum water
136 use varies between individual users within the same user type (Friedman et al. 2013). The
137 minimum pressure head (H_{min}) required is usually determined by water utility standards but in
138 reality can vary across users depending on their subjective perception of the minimum pressure
139 required to perform their individualized water use activities (Mays 2002, City of Toronto 2009,
140 Region of Peel 2010, Denver Water 2012). In this paper, the minimum pressure of approximately
141 30 metres (m) commonly imposed by North American water utilities (City of Toronto, 2009;
142 Region of Peel, 2010; Denver Water, 2012) was used to calculate the minimum mechanical
143 energy.

144 Energy Lost to Friction: The energy lost to friction (*ELTF*) in Equation 6 compares the
145 magnitude of friction loss in the pipe (to satisfy the demand and leakage at the end of the pipe,
146 and demands downstream of the pipe) to the net energy supplied to the pipe. This indicator can
147 be used to characterize the effectiveness of pipe relining, pipe replacement, and leak repair to
148 reduce frictional losses. The metric *ELTF* can range between 0 and 100 percent, where a value of
149 0 percent means that there are no frictional energy losses in the pipe, and a value of 100 percent
150 means that all the net energy supplied to the pipe is lost to friction along the pipe.

$$ELTF = \left(\frac{E_{\text{friction}}}{E_{\text{supplied}} - E_{\text{ds}}} \right) \cdot 100\% \quad (6)$$

Energy Lost to Leakage: The energy lost to leakage (*ELTL*) in Equation 7 compares the magnitude of energy lost to leakage relative to the net energy supplied to the pipe. The leakage term in the numerator includes leak energy, E_{leak}, and the frictional energy loss along the pipe required to meet the leakage flow, Q_l, at the end of the pipe $E_{\text{friction(leak)}}$ (see Table 1). The *ELTL* metric can range between 0 and 100 percent, where a value of 0 percent means that there is no energy loss due to leakage in the pipe and a value of 100 percent means that all the net energy supplied to the pipe is lost to leakage and friction to satisfy the leak in the pipe. The *ELTL* metric can be used to characterize the effectiveness of leakage repair and pressure management in reducing leakage energy loss.

$$ELTL = \left(\frac{E_{\text{leak}} + E_{\text{friction(leak)}}}{E_{\text{supplied}} - E_{\text{ds}}} \right) \cdot 100\% \quad (7)$$

Calculation of Energy Metrics

The pipe-level energy metrics presented above are evaluated by following a number of steps. First, the EPANET2 (Rossman 2000) network solver is used to calculate the hydraulic head at model nodes and pipe flow in model links over a diurnal period. Because the pipe flow direction may change over a day, the hydraulic head at both ends of each pipe are compared at each time step and the node with the higher hydraulic head is identified as the upstream node. Further, to correctly recognize to which pipes a node is an upstream node and to which pipes a node is a downstream node, the mechanical energy that a pipe delivers to the users at its downstream node (multiple-link node) is proportional to its flow rate and is weighted by its flow rate into its corresponding downstream pipes, such that

$$\left(E_{\text{delivered}}\right)_{i,j} = \gamma \left(\frac{Q_i}{\sum_{k=1}^{m} Q_k} \right) D_j H_j \Delta t \quad \text{(joules)} \tag{8}$$

where $(E_{\text{delivered}})_{i,j}$ = energy delivered by pipe i to multiple-link node j (joules); D_j = demand at downstream multiple-link node j located downstream of pipe i (m^3/s); H_j = hydraulic head at multiple-link node j located downstream of pipe i (m); Q_i = flow in pipe i (m^3/s); m = number of $k = 1, 2, 3, \ldots, m$ upstream pipes connected to the multiple-link node j. For example in Figure 2a, upstream pipes P-1 and P-2 with flow rates of 1.3 litres per second (L/s) and 1.6 L/s are connected to downstream node J-1 (multiple-link node) with a demand of 2.1 L/s. Pipes P-3 and P-4 are located downstream of node J-1. The mechanical energy ($\gamma D H \Delta t$) delivered by Pipe 1 is weighted by the ratio of its flow to the total flow conveyed by the upstream pipes, or 1.3/(1.3+1.6).

Once the upstream and downstream nodes of each pipe have been determined, and the energy delivered to each node resolved as described above, the hydraulic heads and pipe flows simulated over the diurnal period are used to calculate the energy components in Table 1 to evaluate the pipe-level metrics in Equations 2-7. An example is shown in Equation 9 where hourly values of $E_{\text{delivered}}$ and E_{supplied} are aggregated together throughout the day to calculate a single value of *GEE* that is representative of the entire day

$$GEE = \left[\frac{(E_{\text{delivered}})_{t=1} + (E_{\text{delivered}})_{t=2} + \ldots + (E_{\text{delivered}})_{t=24}}{(E_{\text{supplied}})_{t=1} + (E_{\text{supplied}})_{t=2} + \ldots + (E_{\text{supplied}})_{t=24}} \right] \cdot 100\% \tag{9}$$

Hydraulic Proximity Indicator

In the following sections of this paper, the proximity of a pipe to a water source is considered as a factor that can influence the energy performance of a pipe. In anticipation of this, an indicator that characterizes the hydraulic proximity of a pipe to a nearby water source is defined in

Equation 10. The hydraulic proximity indicator is based on the general observation that hydraulic head or pipe flow (or both) tend to decrease as one moves away from a water source to the periphery of the system where pipes generally convey smaller flow to downstream users. The hydraulic proximity indicator is a function of the role of the pipe (transmission or distribution) and its location relative to the water source of the system or pressure zone in which it is found. It is important to note that hydraulic proximity is not an indicator of the linear distance that separates a pipe from a water source, but rather an indirect indicator of the proximity of a water main asset to a water source.

$$\text{Proximity Indicator} = Q \cdot H_s \, (m^4 / s) \tag{10}$$

in which Q is the pipe flow (m^3/s) and H_s is the hydraulic head provided at the upstream node of a pipe (m) calculated with the EPANET2.0 hydraulic model. (All heads are calculated according to a fixed datum of 0 m.) High values of the hydraulic proximity indicator as defined in Equation 10 suggest that the water main is located near a water source, whereas low values suggest that the main asset is located away from a water source.

Application of Pipe-Level Metrics to Three Distribution Systems

The new pipe-level metrics were applied to a large *ensemble* of water mains across three distribution systems to examine how system operation and system improvements impinge on the spatial and temporal patterns of energy performance in drinking water mains. System #1 (Figure 2b) is reported in Cabrera et al. (2010) and comprises 14 pipes (40 km), an elevated tank and a pumping station controlled by minimum and maximum tank levels. The system has a total daily demand of 79.8 ML/day with peaks at 8 am (peaking factor of 1.3) and 4 pm (peaking factor of 1.3) (Figure 3). Approximately 15 percent of the total demand is lost to leakage throughout the day. The leakage is assigned to the nodes using emitter coefficients in EPANET2.0 (Cabrera et

al., 2010). Leakage is thus a function of time and pressure. At each time step, EPANET2 is used to calculate pressure head and leakage loss to evaluate the energy lost to leakage (*ELTL*).The average daily pressure in System #1 is approximately 35 m.

System #2 (Figure 4a) is a medium-sized distribution system in the US Midwest that includes 1,183 pipes (166 km), 4 pumping stations and 4 elevated tanks. The water distribution system is comprised of three pressure zones to overcome an elevation difference of 99.7 m to serve a population of 20,000 people. The system has a total daily demand of 237.9 ML/day with an 8 am morning peak (peaking factor of 1.25) and a 10 pm evening peak (peaking factor of 1.67) (Figure 3). The daily mean pressure is 57 m and higher than in System #1. No leakage is considered in this network.

System #3 (Figure 4b) is a large distribution network in the US Midwest that comprises 27,231 pipes (5,500 km), 28 pumping stations, and 27 elevated tanks that serves approximately 1 million customers. This system has a total daily demand of 12,765 ML/day with an 8 am morning peak (peaking factor of 1.18) and a 9 pm evening peak (peaking factor of 1.40). The system has an average nodal pressure of 53 m. Leakage is modelled as a constant demand assigned by area to model nodes based upon the results of a detailed leakage study conducted by the water utility.

Results

System #1

System #1 is a simple system and thus an ideal network with which to demonstrate the new pipe-level metrics by way of two management scenarios (Figure 2b). The first scenario is the Baseline (B) scenario where the pipes are unimproved. The second scenario is the Leakage Reduction (L) scenario where pipe leakage is reduced by 50 percent by reducing emitter

coefficients in the model. In this paper, the energy metrics are dimensionless and expressed as a percentage of i) energy supplied to the pipe ($E_{supplied}$), or ii) minimum energy needed at the downstream node (E_{need}), or iii) the net energy in the pipe ($E_{supplied} - E_{ds}$). For the sake of consistency, numerical values of the metrics that range between 0 and 30 percent are considered "low", while values that range between 30 and 70 percent are considered "moderate", and values that range between 70 and 100 percent are considered "high".

Baseline Scenario (No Improvements): The baseline results in Table 2 indicate that the presence of both frictional losses and leakage in the system produce low to moderate values of *GEE* that range between 8 to 45 percent. This association is evident in the pipes closest to the source and that carry higher flow rates (e.g., pipes 11, 12, 111, and 113) because these pipes must convey flows destined to locations further downstream in the network. Similarly, the presence of leakage in the system produces values of *NEE* that range between 29 to 76 percent.

The results in Table 2 indicate that pipes 22 and 113 have an *ENU* that ranges from 110 to 113 percent. These pipes are located between the tank (dominant source of water in this system) and the highest nodal demand at junction J-22, and thus the large energy surplus reflects the delivery of water to this location from the source. The pipes 31, 121, and 122 located further away from the elevated tank tend to have less surplus energy, and these pipes show an energy deficit and a numerical value of *ENU* that ranges between 91 to 97 percent; these pipes deliver less energy to their users due to water losses between the sources and these demand locations.

The baseline values of *ELTF* suggest that friction losses comprise 39 to 66 percent of net energy in pipes 11 and 111, both of which are in close proximity to the pumping station and carry high flows. Friction comprises 1.3 to 8.0 percent of net energy in the other pipes that convey smaller flows. Also, the results for leakage losses and *ELTL* suggest that pressure and not

leak size (as reflected in the emitter coefficient), drives the level of leakage and results in high values of *ELTL*. For example, even though pipes 113 and 123 both have a low value of emitter coefficient, their proximity to the tank in a high-pressure zone causes them to have a high leakage levels and high values of *ELTL* that range from 18.8 to 22.2 percent.

The results also show that *NEE* in Pipe 121, located far from the tank, is driven almost exclusively by the demand at the downstream node of this pipe (*NEE* = 55 to 61 percent from 12 am to 6 am; *NEE* = 75 to 82 percent from 6 am to 6 pm), whereas the net efficiency in Pipe 11 near the pump is influenced by the pumping and tank operations of the system (*NEE* = 10 to 20 percent during pumping periods of 12 am to 3 am and 1 pm to 5 pm). This finding highlights how the proximity to pumps and tanks and the role of pipes in the global hydraulic performance affects the net efficiency and energy lost to friction observed in individual pipes.

Leakage Reduction Scenario (from 15 to 8 percent of demand): The results for the leakage reduction scenario in Table 2 indicate that reducing leakage flow from 15 to 8 percent produces a 0.2 to 11.0 percent increase in the *GEE* relative to baseline because it narrows the gap between energy delivered and energy supplied. This relationship is especially true for the pipes located further downstream (e.g., pipes 121, 122, 123, 31 and 32). Similarly, all pipes see a 3.9 to 18.8 percent increase in *NEE* relative to baseline as a result of leakage reduction. A reduction in leakage also increases the *ENU* (or reduces the energy deficit) by 1.7 to 10.1 percent relative to baseline because energy lost to leakage is decreased in the pipes. In most pipes, a reduction in leakage is tantamount to reduced pipe flow and therefore less energy lost to leakage and friction. For example, a reduction in leakage produces a 0.8 to 8.0 percent decrease in *ELTF* in pipes 112, 113, and 121 relative to baseline. However, in smaller pipes located further downstream in the system (e.g., pipes 31, 32), the friction losses tend to increase because of an increase in pipe

flow–a result of reduction in leakage between the water source and these pipes. Lastly, a reduction in leakage causes a 47.2 to 57.3 percent decrease in *ELTL* in all pipes.

System #2

In System #2, the energy metrics were evaluated only for those pipes (approximately 600 pipes or 60 percent of the total number of pipes) that have a non-zero downstream demand. Because leakage was not modelled for this system, only metrics *GEE, NEE, ENU,* and *ELTF* were evaluated for the baseline scenario; the impact of interventions such as leakage reduction on energy dynamics was not considered. System #2 was simulated with assumed leakage levels (no leakage, 15 percent, 30 percent) and the results (not shown) suggest that the presence of leakage produces a similar frequency distribution of the numerical values of the four energy metrics as shown in Figures 5 and 9. The absence of leakage data for System #2 does not preclude the comparison of energy dynamics in System #2 with the other two systems (Systems #1 through #3).

The histogram results in Figure 5 show that the *GEE* follows a bimodal distribution. Here, over 60 percent of the pipes have a low value of *GEE* that ranges from 0 to 10 percent while approximately 14 percent of the pipes have a high value of *GEE* that ranges from 90 to 100 percent. It is noted that low values of *GEE* in Figure 6a do not necessarily point to a poor energy performance as these pipes tend to be located near the major system components and supply a large number of users downstream. Pipes with a high *GEE* tend to be located near dead-end zones where most of the energy supplied to the pipe is used to satisfy demand at the downstream node of the pipe. Over 90 percent of the pipes have a *NEE* that ranges from 90 to 100 percent (Figure 5). Figure 6b indicates that there are trunk mains and distribution mains near pumps and tanks with low to high values of net efficiency (0.1 to 80 percent).

303 The majority of pipes (almost 80 percent) exhibit a low *ELTF* between 0 and 10 percent
304 (Figure 5). However a minority of pipes (almost 15 percent) had high frictional energy losses,
305 with *ELTF* between 90 and 100 percent. These pipes are large-diameter trunk mains that carry
306 large flows with a high average unit headloss, and are located in close proximity to a pump or
307 tank. (In this paper, average unit headloss is calculated by taking the arithmetic average of unit
308 headloss in a pipe over the 24-hour diurnal period.)
309 The energy performance of two representative pipes (Pipes 463 and 926 – see Figures 4a
310 and 6) during the 24-hour diurnal period was also examined (Figure 7). Pipe 463 is a 300 mm CI
311 water main located near pumping station P1 in System #2 and conveys flows between 15-86 L/s
312 throughout the service day. Not surprisingly, the *ELTF* in Pipe 463 varies in lockstep with the
313 flow in the pipe, whereby *ELTF* varies between 0.1 to 3 percent during low-demand periods
314 and *ELTF* varies between 5 to 27 percent during high-demand periods. The net energy efficiency
315 in Pipe 463 varies widely during the 24-hour diurnal period, with values of *NEE* between 72 and
316 86 percent during high-demand periods and values between 92 to 100 percent during low-
317 demand periods. By contrast, Pipe 926 is a 150 mm CI main located near the periphery of the
318 system (Figure 4a). This pipe conveys a near-constant flow of less than 0.10 L/s. Not
319 surprisingly, *ELTF* is correspondingly low (near 0 percent throughout the whole day in Figure 7)
320 and the net energy efficiency of this pipe is at a near-constant level of 100 percent. The results
321 suggest that the energy performance (in this case efficiency and friction) of a pipe is contingent
322 on the proximity of that pipe to a pump or tank.
323 The influence of the distance between a pipe and a major component on the energy performance
324 of that pipe was examined further. This was done by plotting *ELTF* calculated with Equation 6
325 and the max/min hourly value of energy lost to friction (*ELTF*-max, *ELTF*-min, Equation 9)

observed over the 24-hour diurnal period against the hydraulic proximity indicator (Equation 10) in Figure 8 for an *ensemble* of 684 pipes. The results suggest that *ELTF* is smaller in distribution mains located further away from water sources that convey low flows and incur small losses (*ELTF*-min near 0 percent). Pipes located close to water sources tend to have a value of *ELTF*-max of 100 percent (this occurs during the peak demand period). Figure 8 shows a high variation in *ELTF*-max in pipes located far away from water sources. This variability is likely owing to differences in diameter, roughness, and service flows across the smaller water distribution mains located on the periphery.

System #3

The energy metrics were evaluated for over 21,000 pipes, which represents approximately 77 percent of pipes in System #3. In general, the findings for System #3 are similar to those for System #2 in that the frequency distribution of the numerical values of metrics follows a bimodal shape (Figure 9). The bimodal nature of the results emphasizes the variability of energy performance in complex systems when compared to a simpler system like System #1. The majority of pipes exhibit a good energy performance (high net energy efficiency, small frictional losses) and a minority of outlier pipes exhibit a poor energy performance (low efficiency, high losses).

The histogram in Figure 9 indicates that approximately 80 percent of pipes have a value of *GEE* that ranges between 0 and 20 percent. As noted before, low values of *GEE* do not necessarily point to a poor energy performance; in these trunk pipes the majority of the energy supplied to the pipe is transferred to users well downstream of the pipe and only a small fraction of the energy is delivered to users at the end of the pipe. Figure 9 also indicates that 2 percent of pipes have a value of *GEE* that ranges between 90 and 100 percent. In these distribution mains

near cul-de-sac areas, most of the energy is transferred to users directly at the end of the pipe. Approximately 90 percent of pipes have a *NEE* that ranges between 9 and 100 percent (Figure 9) but a minority of pipes (4 percent) have a low to moderate net energy efficiency that ranges between 10 and 50 percent. A detailed analysis showed that no single factor accounted for the low values of net energy efficiency in these pipes.

More than 95 percent of pipes have an *ENU* that ranges between 100 and 120 percent (Figure 9) and over 90 percent of pipes have a low *ELTF* that ranges between 0 and 10 percent. Leakage performance for this system is good with over 95 percent of pipes having a low *ELTL* that ranges between 0 and 10 percent. Despite this generally good performance, there are a small number of outlier pipes (approximately 3 percent of total) with a moderate to high *ELTF* that ranges between 40 and 100 percent. Many of these poorly performing pipes were found to be large-diameter trunk mains that convey large flows from water sources to the rest of the system. A small number of pipes (2.5 percent of total) were also found to have a moderate to high *ELTL* that ranges between 40 and 100 percent, and this is a direct result of the assigned leakage values from the water utility leakage study.

The diurnal variation of *NEE* and *ELTF* in select pipes of System #3 were examined (results not shown). As before, the results suggest that proximity to a water source and magnitude of pipe flow conveyed by the pipe are both factors that have a large impact on the diurnal variation of net energy efficiency and energy lost to friction. Generally, pipes located far away from water sources convey little flow (with small headloss) and have values of *NEE* near 100 percent and *ELTF* near 0 percent throughout the day. In larger trunk mains located closer to water sources with comparatively high flow rates, *NEE* and *ELTF* track closely with diurnal variations in pumped flow in these pipes, as was also observed in System #2.

The influence of the distance between a pipe and a major component on the energy performance of that pipe was examined in System #3. Figure 10 plots the *ELTL* and the max/min value of energy lost to leakage (*ELTL*-max and *ELTL*-min over a 24-hour period) for each pipe (y-axis) against the hydraulic proximity indicator (x-axis). The values of the energy loss metrics *ELTL*, *ELTL*-max, and *ELTL*-min are moderate (30 to 60 percent) near water sources (proximity ranges between 3,000 and 6,000 m^4/s) and moderate to high (30 to 100 percent) at the periphery of the system (proximity ranges between 0 and 250 m^4/s). This relationship can be explained by two factors: 1) the trunk water mains close to a water source have a low level of leakage while the smaller distribution mains near the periphery of the system have a higher level of leakage, and 2) the values of net energy supplied to the pipe ($E_{supplied} - E_{ds}$, denominator of *ELTL*) are large and outweigh the energy lost due to leaks ($E_{leakage} + E_{friction(leak)}$, numerator of *ELTL*) because of the low level of leakage at locations near water sources. There is also a high degree of variability in the values of *ELTL* and *ELTL*-max near the periphery of the system as shown in Figure 10 (proximity ranges between 0 and 250 m^4/s).

Comparison of Energy Metrics With Average Unit Headloss and Pressure Head

The usual practice is to use average unit headloss to identify pipes with high frictional line losses and pressure head (or excess pressure head) to identify which pipes are delivering excess mechanical energy to customers. Here, the energy lost to friction (*ELTF*) was compared to average unit headloss to assess their effectiveness in identifying pipes with high frictional energy losses. To do this, the five pipes with the highest values of *ELTF* and the five pipes with the highest values of average unit headloss were selected from the *ensemble* of 1,183 pipes in System #2 and their corresponding annual frictional energy loss was calculated. (Annual frictional energy loss was calculated by multiplying the frictional energy loss in a pipe over the

24-hour diurnal period and multiplying this daily energy use by 365 days.) This was repeated for System #3 (*ensemble* of 21,156 pipes). The results in Table 3 indicate the five pipes with the highest values of *ELTF* and average unit headloss sorted in descending order of annual frictional energy loss. Table 3 indicates that in System #2, *ELTF* and average unit headloss identified the same four pipes (69, 159, 117, 41) with the highest annual frictional energy loss, and in System #3, *ELTF* and average unit headloss both identified pipe 3464 as having the highest annual frictional energy loss. It it noted that average unit headloss identified four pipes with higher annual frictional energy loss than the *ELTF*. A possible reason for this is that average unit headloss relates more directly to annual frictional energy loss than *ELTF*.

In Table 4, the energy needed by user (*ENU*) and energy lost to leakage (*ELTL*) were compared to pressure head to determine their effectiveness in identifying pipes that experience the highest energy losses to leakage. Similar to the above, the five pipes with the highest values of *ENU* and the highest values of pressure head were selected from the *ensemble* of pipes in System #3 and sorted in descending order of annual energy lost to leakage. (Annual energy lost to leakage was calculated by multiplying the leak energy at the downstream node of a pipe over the 24-hour diurnal period and multiplying this daily energy use by 365 days.) The results in Table 4 suggest that the pipes identified with *ENU* and *ELTL* had higher values of annual energy lost to leakage than those identified with pressure head. The metrics of gross energy efficiency (*GEE*) and net energy efficiency (*NEE*) were not compared to average unit headloss and pressure head. The interested reader can find the model data and the implementation code for the new energy metrics in the supplemental data files appended to this manuscript.

Discussion

Previous research has shown that reducing leakage flow in distribution systems produces a corresponding reduction in energy use (Colombo and Karney 2002, 2005). Cabrera et al. (2010) found that leak-free systems required less energy per cubic metre of water delivered. Not surprisingly, the observations made in System #1 of this paper corroborate these observations, whereby a 50 percent reduction in leakage flow produced a near proportional decrease in energy lost to leakage and improved gross and net efficiency and reduced energy lost to friction. Additional observations on more realistic and more complex systems are needed to verify that this near one-to-one relationship holds for most systems.

The analysis of Systems #2 and #3 showed that the statistical distribution of energy performance of the pipes in these two large systems is bimodal where the majority of pipes have a good energy performance (high efficiency, low energy losses) but that an important minority of outlier pipes also have a poor energy performance (low efficiency, high energy losses to friction and leakage). The research of Dziedzic and Karney (2014) showed an asymmetrical energy performance across the Toronto distribution system such that water mains immediately downstream of treatment works had higher energy dissipation rates than pipes located further away from treatment plants. The results of the current paper corroborate this previous finding. In all three systems examined, pipes near components tended to have low gross and net efficiencies and high energy losses due to friction and leakage, while pipes located far away from components had high gross and net efficiencies and low friction and leakage losses. Pipes near components that experienced surplus pressures generally met the minimum energy needed by the users ($ENU > 100$ percent) even if their *ELTL* was generally high. However, pipes in lower-pressure regions further away from components generally fell short of meeting the minimum

energy needed by the users (*ENU* < 100 percent) and showed lower energy losses to leakage.

The findings of this paper showed that there is also a strong diurnal variation in energy inputs and outputs at the scale of the individual pipe. For all systems examined, the diurnal variation of energy efficiency and energy lost to friction in pipes close to components tended to be influenced heavily by pumping periods and tank-draining periods when pipe flows and losses were high in these pipes. Diurnal variation of energy efficiency and energy lost to friction in pipes located far away from components tended to be more influenced by diurnal variation in demand. These pipes had a low efficiency and high frictional losses during high-demand periods and high efficiency and low frictional losses during low-demand periods. These finding support the previous research that showed wide diurnal variations in global energy efficiencies in the Toronto distribution system, where low frictional losses and high efficiencies were observed in the night time when demand was low (Dziedzic and Karney 2014).

The results of this study also showed that the new metrics of *ELTF*, *ENU*, and *ELTL* may be complementary indicators of energy performance in a pipe to the traditional indicators of average unit headloss and pressure head. The results showed that the average unit headloss was on the whole more successful than the *ELTF* metric in identifying pipes with the highest annual energy frictional losses. This shows that average unit headloss is still an important measure because it is directly tied to the pumping costs borne by a water utility. Nevertheless, the *ELTF* metric could be used to evaluate the contribution of frictional losses relative to energy lost to leakage and energy lost at the point of demand in pipes selected for rehabilitation with the average unit headloss variable. Arguably, this could help water utilities understand the relative importance of friction in the context of other energy losses in their system.

The results also suggested that the *ENU* and *ELTL* metrics are more successful than pressure

head in identifying the pipes that have the greatest energy losses to leakage. This is because *ENU* and *ELTL* account for both flow and pressure head at the point of leakage that drive the mechanical energy that exits the system. These results suggest that *ENU* and *ELTL* have the potential to be good indicators of energy lost to leakage in distribution systems. However, the results of System #1 suggest that it is the pipes that have both high pressure and high leakage flow which tend to have the highest energy loss to leakage. For this reason, the results of this study suggest that pressure head or leakage flow alone are not good indicators of energy lost to leakage.

While the location of the pipe in the system has been found to have an important influence on energy use, there are likely synergistic effects between the proximity to a water source and other factors such as pipe diameter, pipe flow, leakage level, unit headloss that work together to determine energy performance in a pipe. This paper did not examine the underlying, combined effects of these key factors on the energy performance of pipes.

In order for the metrics of this paper to provide an accurate picture of energy performance in water mains, a calibrated network model is needed with good pipe data (e.g., wall roughness and diameter) and good data on the magnitude and spatial distribution of leakage. It is noted that many municipalities in Canada and the US do not have good spatially-disaggregated data on leakage and pipe roughness/diameter in their typically large pressure zones. Increasingly, these municipalities are quantifying leakage levels and pipe flows by metering small well-defined DMA (district metering area) areas that are smaller in size than traditional pressure zones. DMA sectorization and flow/leak monitoring is already well-established in European countries and other parts of the world and the metrics can be applied with good accuracy in these jurisdictions.

Conclusion

Previous research has shown the usefulness of energy metrics to examine the global or system-wide energy performance of water distribution systems (Cabrera et al. 2010; Cabrera et al. 2014a, 2014b; Dziedzic and Karney 2014) and the balance between inputs and outputs of energy through friction and leakage losses. The current paper offered a complementary approach in the form of novel metrics that resolve energy performance at the spatial scale of the individual water main. The results of the paper showed that average unit headloss is on the whole more successful than *ELTF* in identifying pipes with high frictional energy losses, but that the new *ENU* and *ELTL* metrics are more successful than pressure head in identifying pipes that experience the highest energy losses to leakage. These metrics have the potential to assist water utilities in understanding the energy performance of unimproved pipes alongside cost, structural and water quality concerns. While outside the scope of this paper, water utilities can potentially leverage this pipe-level energy analysis to perform life-cycle costing that compares the cost of pipe rehabilitation against the surplus energy cost (from leakage and frictional losses) incurred in a pipe when not rehabilitated (do-nothing option) to characterize the payback period of the rehabilitation intervention.

Acknowledgements

The authors wish to thank the Natural Science and Engineering Research Council for its financial support of this research. Dr. Speight received support from the Engineering and Physical Sciences Research Council under grant EP/I029346/1. The authors also thank Mr. Brett Snider from the Department of Civil Engineering, Queen's University for his helpful comments that contributed to the progress of this research.

References

Alvisi, S., & Franchini, M. (2006). Near-optimal rehabilitation scheduling of water distribution systems based on a multi-objective genetic algorithm. *Civil Engineering and Environmental Systems*, 23(3), 143-160.

Alvisi, S., & Franchini, M. (2009). Multiobjective optimization of rehabilitation and leakage detection scheduling in water distribution systems. *Journal of Water Resources Planning and Management*, 135(6), 426-439.

American Water Works Association (2009). *M36 Water Audit and Loss Control Programs*. American Water Works Association, Denver, Colorado, pp. 422.

American Water Works Association (1991). *M32 Distribution Network Analysis for Water Utilities*. American Water Works Association, Denver, Colorado, pp. 39.

Askew, L.E., and McGuirk, P.M. (2004). "Watering the suburbs: distinction, conformity and the suburban garden." *Australian Geographer*, *35*(1), 17-37.

Boulos, P. F., Lansey, K. E., Karney, B. W. (2006). *Comprehensive Water Distribution Systems Analysis Handbook for Engineers and Planners*, MWHSoft Press, Pasadena, CA, USA.

Cabrera, E., Pardo, M.A., Cobacho, R., and Cabrera Jr., E. (2010). "Energy audit of water networks." *Journal of Water Resources Planning and Management*, 136(6), 669-667.

Cabrera, E., Gómez, E., Cabrera Jr, E., Soriano, J., and Espert, V. (2014a). "Energy Assessment of Pressurized Water Systems." *Journal of Water Resources Planning and Management*, 141(8), 04014095: 1-12.

Cabrera, E., Cobacho, R., and Soriano, J. (2014b). "Towards energy labeling of pressurized water networks." *Procedia Engineering*, 70, 209-217.

City of Toronto (2009). *Design criteria for sewers and water mains*. Engineering and

530 Construction Services, Toronto, Ontario, Canada.
531 Colombo, A.F., and Karney, B.W. (2002). "Energy cost of leaky pipes: Toward a
532 comprehensive picture." *Journal of Water Resources Planning and Management*, 128(6), 441-
533 450.
534 Colombo, A.F., and Karney, B.W. (2005). "Impacts of leaks on energy consumption in
535 pumped systems with storage." *Journal of Water Resources Planning and Management*, 131(2),
536 146-155.
537 Dandy, G. C., & Engelhardt, M. (2001). Optimal scheduling of water pipe replacement using
538 genetic algorithms. *Journal of Water Resources Planning and Management*, 127(4), 214-223.
539 Denver Water (2012). Engineering Standards 14th Ed., Denver, Colorado.
540 Dziedzic, R., & Karney, B. W. (2015). Energy Metrics for Water Distribution System
541 Assessment: Case Study of the Toronto Network. *Journal of Water Resources Planning and*
542 *Management*, 141(11), 04015032.
543 Dziedzic, R. M., and Karney, B. W. (2014). "Water Distribution System Performance
544 Metrics." *Procedia Engineering*, 89, 363-369.
545 Fontana, N., Giugni, M., & Portolano, D. (2011). Losses reduction and energy production in
546 water-distribution networks. *Journal of Water Resources Planning and Management*, 138(3),
547 237-244.
548 Friedman, K., Heaney, J., Morales, M., and Palenchar, J. (2011). "Water Demand
549 Management Optimization Methodology." *Journal of American Water Works Association*,
550 103(9), 74-84.
551 Friedman, K., Heaney, J. P., Morales, M., and Palenchar, J. E. (2013). "Predicting and
552 managing residential potable irrigation using parcel-level databases." Journal of American Water

553 Works Association, 105(2), 372–386.
554 Hashemi, S.S., Tabesh, M., and Ataee Kia, B. (2013). Scheduling and operating costs in
555 water distribution networks. *Journal of Water Management*, 166 (8), 432–442.
556 Hoekstra, A. Y., and Chapagain, A. K. (2007). "Water footprints of nations: water use by
557 people as a function of their consumption pattern." Water Resources Management, 21(1), 35-48.
558 Kleiner, Y., & Rajani, B. (2001). Comprehensive review of structural deterioration of water
559 mains: statistical models. *Urban water*, 3(3), 131-150.
560 Lambert, A. O., Brown, T. G., Takizawa, M., & Weimer, D. (1999). A review of
561 performance indicators for real losses from water supply systems. *Journal of Water Supply:*
562 *Research and Technology-Aqua*, 48(6), 227-237.
563 Mayer, P. and DeOreo, W. (2010). "Improving Urban Irrigation Efficiency by Using
564 Weather-based Smart Controllers." *Journal of American Water Works Association,* 102(2), 86-
565 97.
566 Mays, L. (2002). *Urban Water Supply Handbook.* McGraw-Hill, New York, NY.
567 Morales, M., Heaney, J., Friedman, K., and Martin, J. (2011). "Estimating Commercial,
568 Industrial, and Institutional Water Use on the Basis of Heated Building Area." *Journal of*
569 *American Water Works Association,* 103(6), 84-96.
570 Pelli, T., and Hitz, H. U. (2000). "Energy indicators and savings in water supply." *Journal of*
571 *American Water Works Association*, *92*(6), 55-62.
572 Region of Peel (2010). Public Works Design, Specifications and Procedures Manual. Region
573 of Peel, Mississauga, Ontario, Canada.
574 Roshani, E., & Filion, Y. R. (2013). Event-based approach to optimize the timing of water
575 main rehabilitation with asset management strategies. *Journal of Water Resources Planning and*

Management, 140(6), 04014004.

Rossman, L.A. (2000). EPANET2*: User's Manual*. *US Environmental Protection Agency*. Cincinnati, OH.

Vickers, A. (2001). *Handbook of Water Use and Conservation*. Water Plow Press. Amherst, Massachusetts.

582 Table 1. Energy inputs and outputs linked to fluid flow in a pipe.

583 Table 2. Numerical values of metrics *GEE, NEE, ENU, ELTF,* and *ELTL* for the baseline and
584 leakage reduction scenarios in System #1 (reported in Cabrera et al. (2010). *GEE:* Gross Energy
585 Efficiency; *NEE:* Net Energy Efficiency*; ENU:* Energy Needed by User; *ELTF:* Energy Lost to
586 Friction; *ELTL:* Energy Lost to Leakage.

587 Table 3. Pipes with the highest values of average unit headloss and energy lost to friction (*ELTF)*
588 in System #2 (*ensemble* of 1,183 pipes) and System #3 (*ensemble* of 21,156 pipes). (Pipes are
589 sorted by annual frictional energy loss in descending order.)

590 Table 4. Pipes with the highest values of pressure, energy needed by user (*ENU*), and energy lost
591 to leakage (*ELTL*) in System #3 (*ensemble* of 21,156 pipes). (Pipes are sorted by annual energy
592 lost to leakage in descending order.)
593

Table 1.

Energy Components	Equations
Energy supplied	$E_{supplied} = \gamma Q H_s \Delta t$
Energy delivered	$E_{delivered} = \gamma Q_d H_d \Delta t$
Minimum energy needed to meet the end-user demand in an pipe	$E_{need} = \gamma Q_d H_{min} \Delta t$
Energy that flows out of pipe to meet downstream demands	$E_{ds} = \gamma Q_{ds} H_d \Delta t$
Leak energy	$E_{leak} = \gamma Q_l H_d \Delta t$
Energy lost to friction to meet demand	$E_{friction(demand)} = \gamma [K (Q_d)^{\alpha}] Q_d \Delta t$
Energy lost to friction to meet leakage	$E_{friction(leak)} = \gamma [K (Q_l)^{\alpha}] Q_l \Delta t$
Energy lost to friction (meet d/s demand)	$E_{friction(ds)} = \gamma [K (Q_{ds})^{\alpha}] Q_{ds} \Delta t$, where $Q_{ds} = Q - Q_d - Q_l$

607 Table 2.

Pipe	GEE (percent)		NEE (percent)		ENU (percent)		ELTF (percent)		ELTL (percent)	
	B	**L**	**B**	**L**	**B**	**L**	**B**	**L**	**B**	**L**
11	8	9	29	29	103	106	66	68	4	2
12	8	8	52	52	106	108	39	42	7	3
113	22	23	73	73	110	115	8	8	19	9
123	42	47	70	70	101	111	4	4	22	11
111	22	24	48	48	103	108	39	40	10	5
121	45	48	73	73	97	104	5	5	14	7
122	43	47	72	72	91	98	2	2	18	9
22	37	37	76	76	113	116	6	7	9	5
21	33	35	75	75	104	109	5	6	12	6
31	37	39	73	73	95	102	1	2	15	7
32	42	45	71	71	104	112	2	2	18	9
112	33	36	74	74	106	111	7	7	15	7

608 B = baseline scenario; L = leakage reduction scenario.

609

Table 3.

Pipe ID	Average Unit Headloss (m/km)[c]	Annual Frictional Energy Loss (MWh)[d]	Pipe ID	*ELTF* (Percent)[e]	Annual Frictional Energy Loss (MWh)[d]
		System #2			
69[a]	470.8	2,971.6	69[a]	99.9*[f]	2,971.5
159	277.1	963.3	159	99.9*	963.3
431	131.3	644.4	117	99.9*	178.8
117	88.9	178.8	41	99.9*	150.0
41	478.2	150.0	P-97	99.9*	59.9
		System #3			
3464[b]	3.9	39,552.0	3464[b]	99.9*[f]	39,552.0
26688	2.3	28,081.6	10959	99.9*	1,313.0
9706	0.1	3,908.0	8735	99.9*	894.7
10942	0.2	1,804.4	11236	99.9*	326.0
11209	0.1	1,097.2	26528	99.9*	307.3

a. Pipes with the highest average unit headloss and energy lost to friction (*ELTF*) in the *ensemble* of 1,183 pipes in System #2 were sorted by annual frictional energy loss in descending order.

b. Pipes with the highest average unit headloss and energy lost to friction (*ELTF*) in the *ensemble* of 21,156 pipes in System #3 were sorted by annual frictional energy loss in descending order.

c. Average unit headloss was calculated by taking the arithmetic average of hourly values of unit headloss in a pipe over the 24-hour diurnal period.

d. Annual frictional energy loss was calculated by multiplying the frictional energy loss in a pipe over the 24-hour diurnal period and multiplying this daily energy use by 365 days.

e. Energy lost to friction (*ELTF*) was calculated by taking the arithmetic average of hourly values of *ELTF* in a pipe over the 24-hour diurnal period.

f. Numerical values of *ELTF* were truncated to the tenth of a percent in the table.

Table 4.

Pipe ID[a]	Average Pressure Head (m)[b]	Annual Energy Lost to Leakage (MWh)[g]	Pipe ID[a]	Metric (Percent)	Annual Energy Lost to Leakage (MWh)[g]
Metric: *ENU*[c,d]					
14509	94.3	10.5	6873	123.0	17.5
14510	91.9	10.3	3443	123.4	15.8
P1379	163.1	7.3	19728	122.4	8.3
10942	92.3	6.3	19729	122.8	7.7
26572	98.8	5.3	6882	123.1	7.5
Metric: *ELTL*[e,f]					
14509	133.4	10.5	9540	99.0	52.2
14510	130.0	10.3	11538	97.4	15.5
19729	124.3	7.7	5898	97.8	15.2
10942	130.5	6.3	P423	99.5	11.1
19732	125.6	6.1	5877	100.0	10.2

a. Pipes with the highest average pressure head in the *ensemble* of 21,156 pipes in System #3 were sorted by annual energy lost to leakage in descending order.

b. Average pressure head was calculated by taking the arithmetic average of hourly pressure head values in the upstream and downstream nodes of a pipe over the 24-hour diurnal period.

c. Energy needed by user (*ENU*) was calculated by taking the arithmetic average of hourly *ENU* values in a pipe over the 24-hour diurnal period.

d. Pipes with the highest energy needed by user (*ENU*) in the *ensemble* of 21,156 pipes in System #3 were sorted by annual energy lost to leakage in descending order.

e. Energy lost to leakage (*ELTL*) was calculated by taking the arithmetic average of hourly *ELTL* values in a pipe over the 24-hour diurnal period.

f. Pipes with the highest energy lost to leakage (*ELTL*) in the *ensemble* of 21,156 pipes in System #3 were sorted by annual energy lost to leakage in descending order.

g. Annual energy lost to leakage was calculated by multiplying the leak energy (E_{leak} indicated in Table 1) at the downstream node of a pipe over the 24-hour diurnal period and multiplying this daily energy use by 365 days.

Figure 1

Click here to download Figure Figure 1.tif

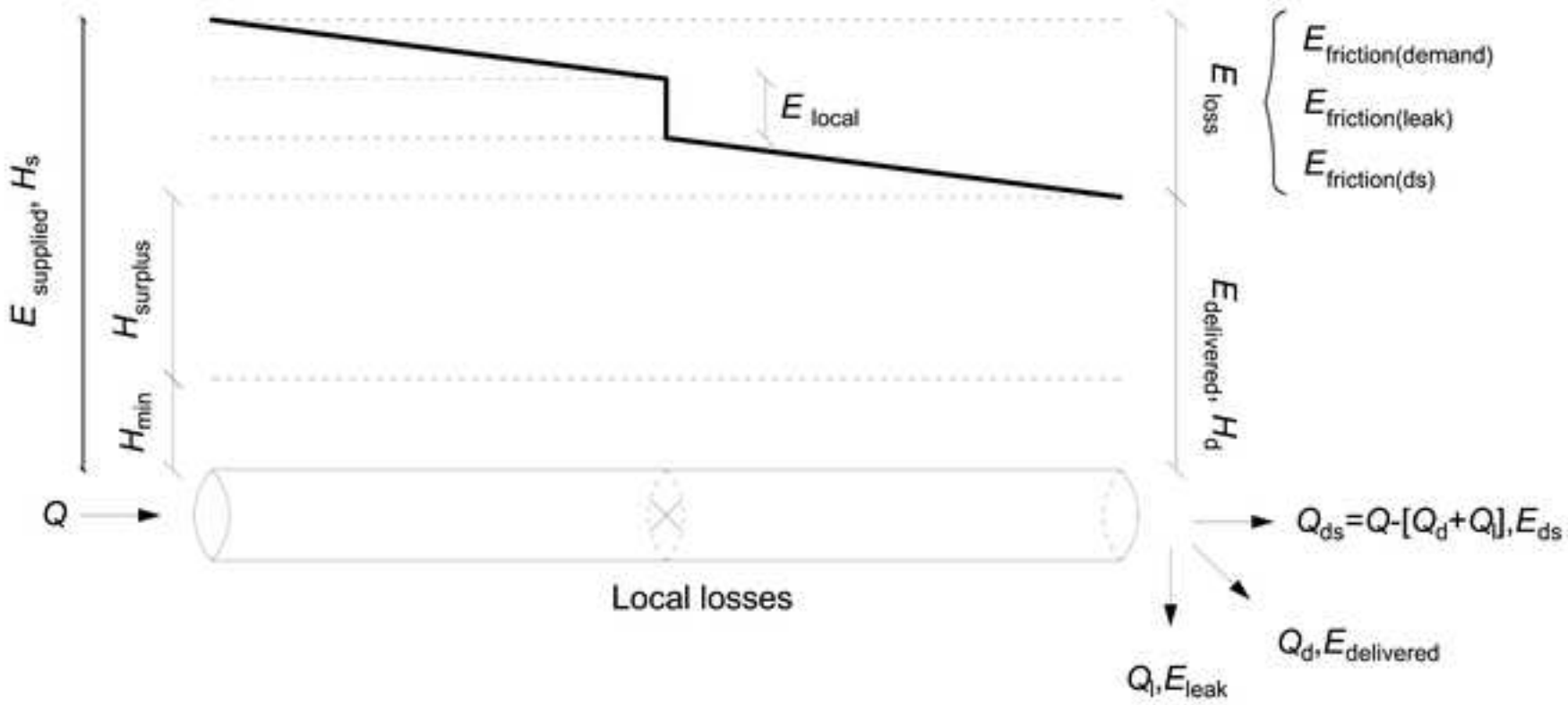

Figure 2a and 2b

Click here to download Figure Figure 2 ab.tif

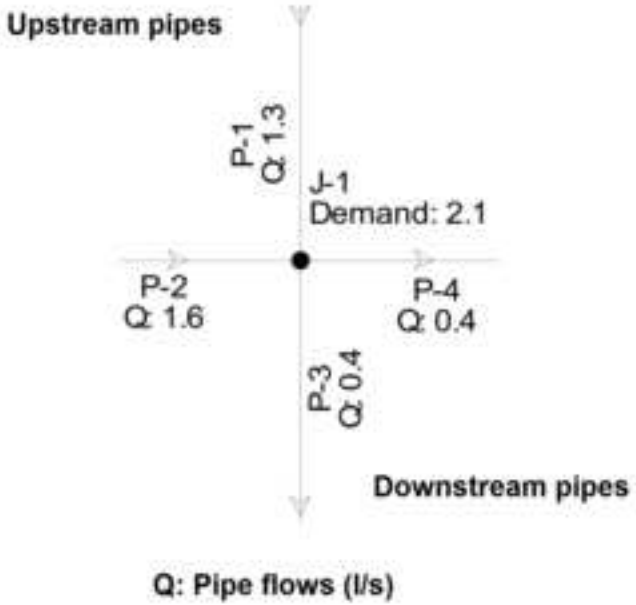

(a)

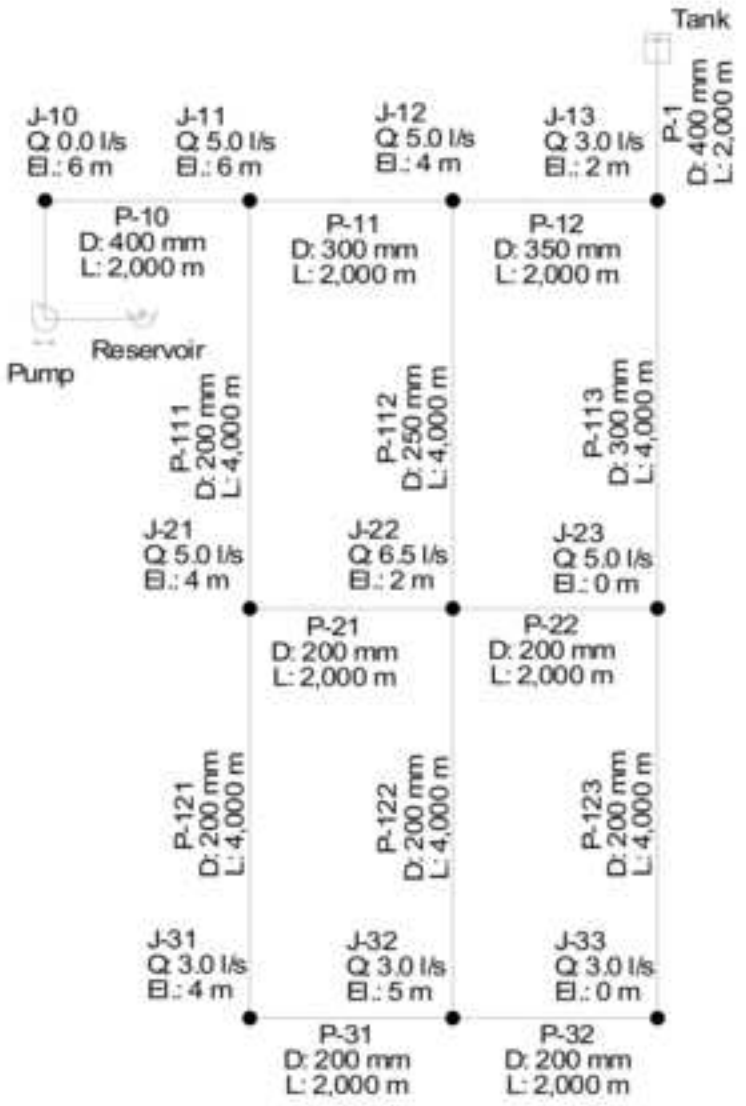

(b)

Figure 3

Click here to download Figure Figure 3.pdf

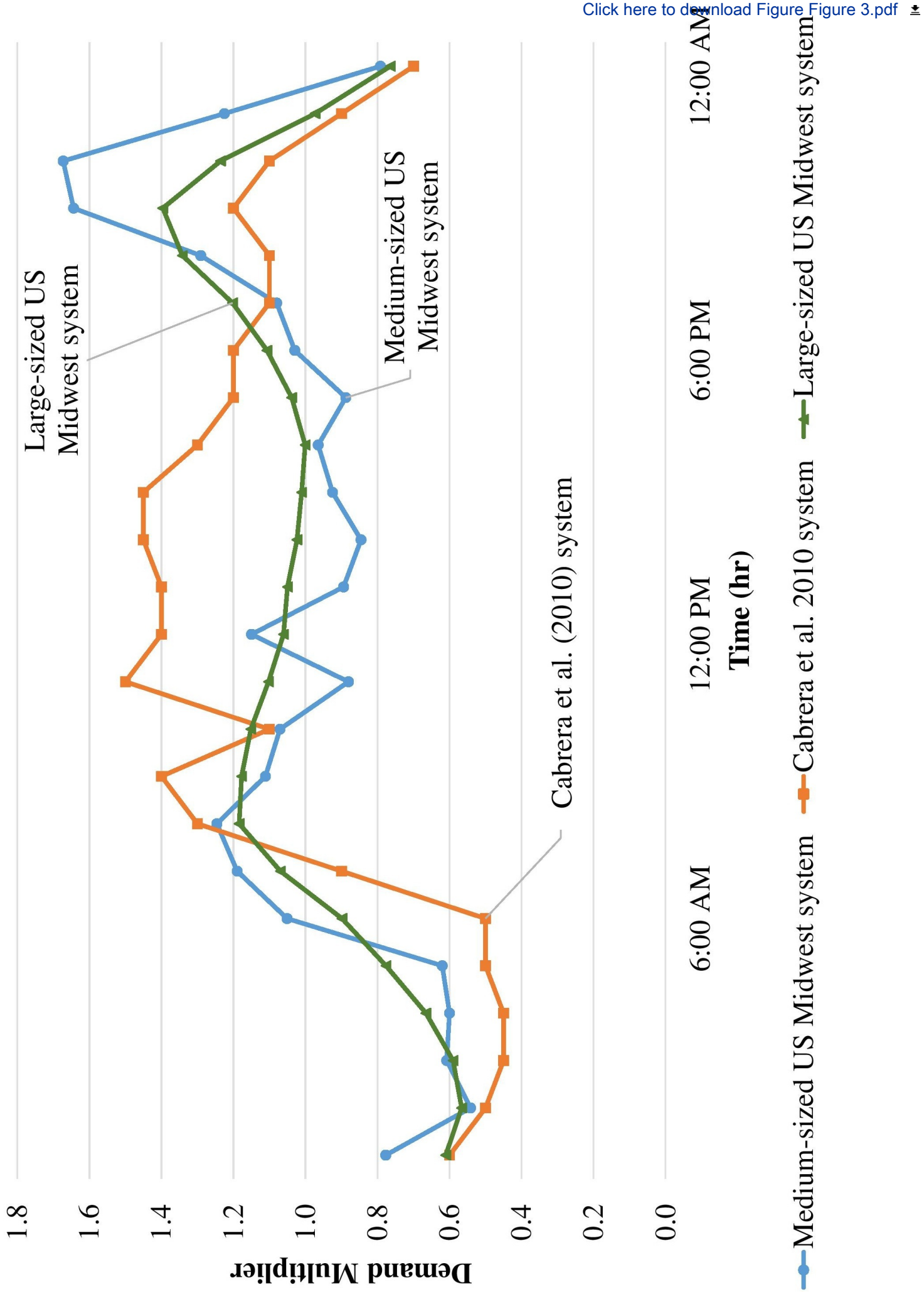

Figure 4a

Click here to download Figure Figure 4a.tif

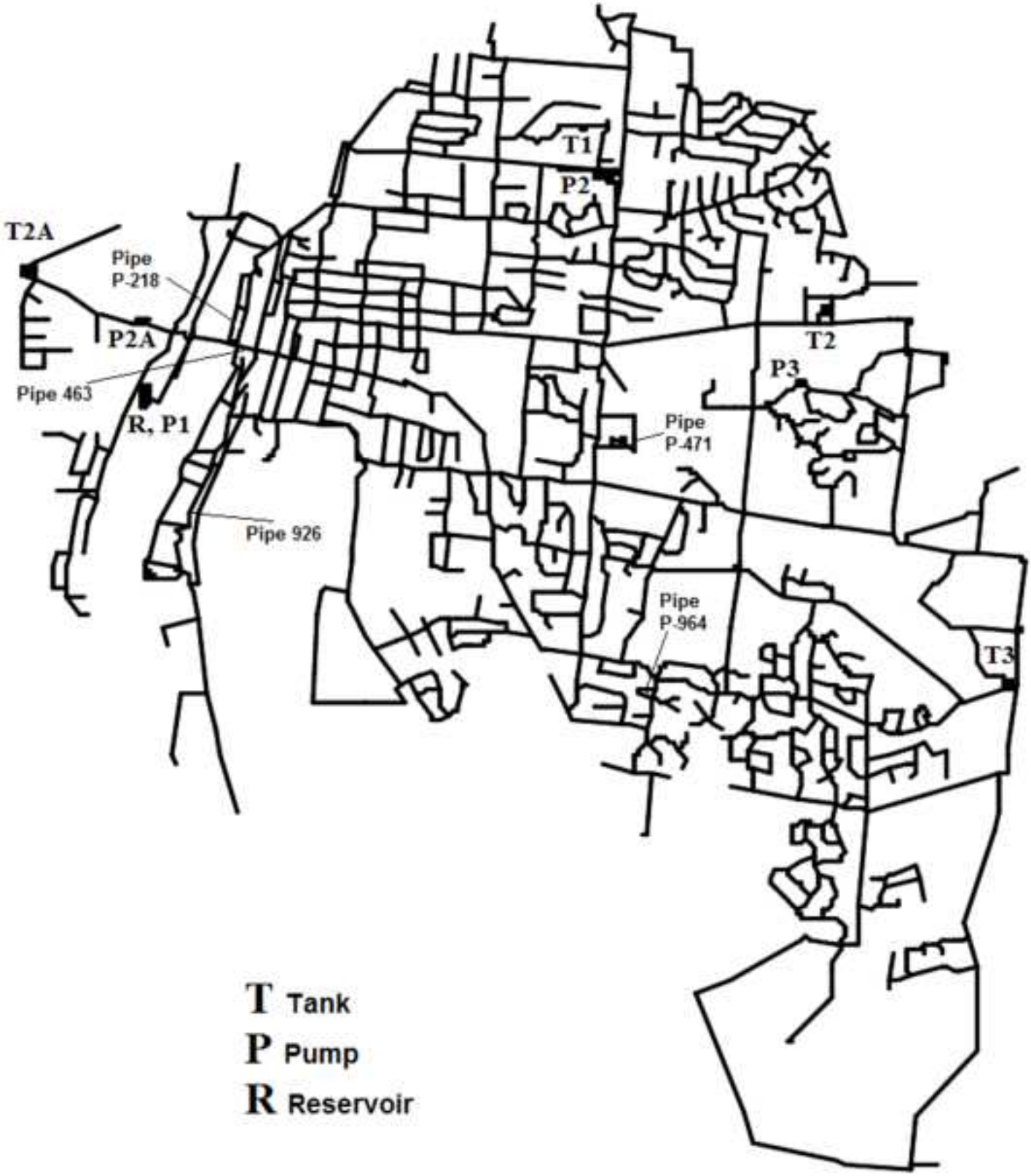

Figure 4b

Click here to download Figure Figure 4b.pdf

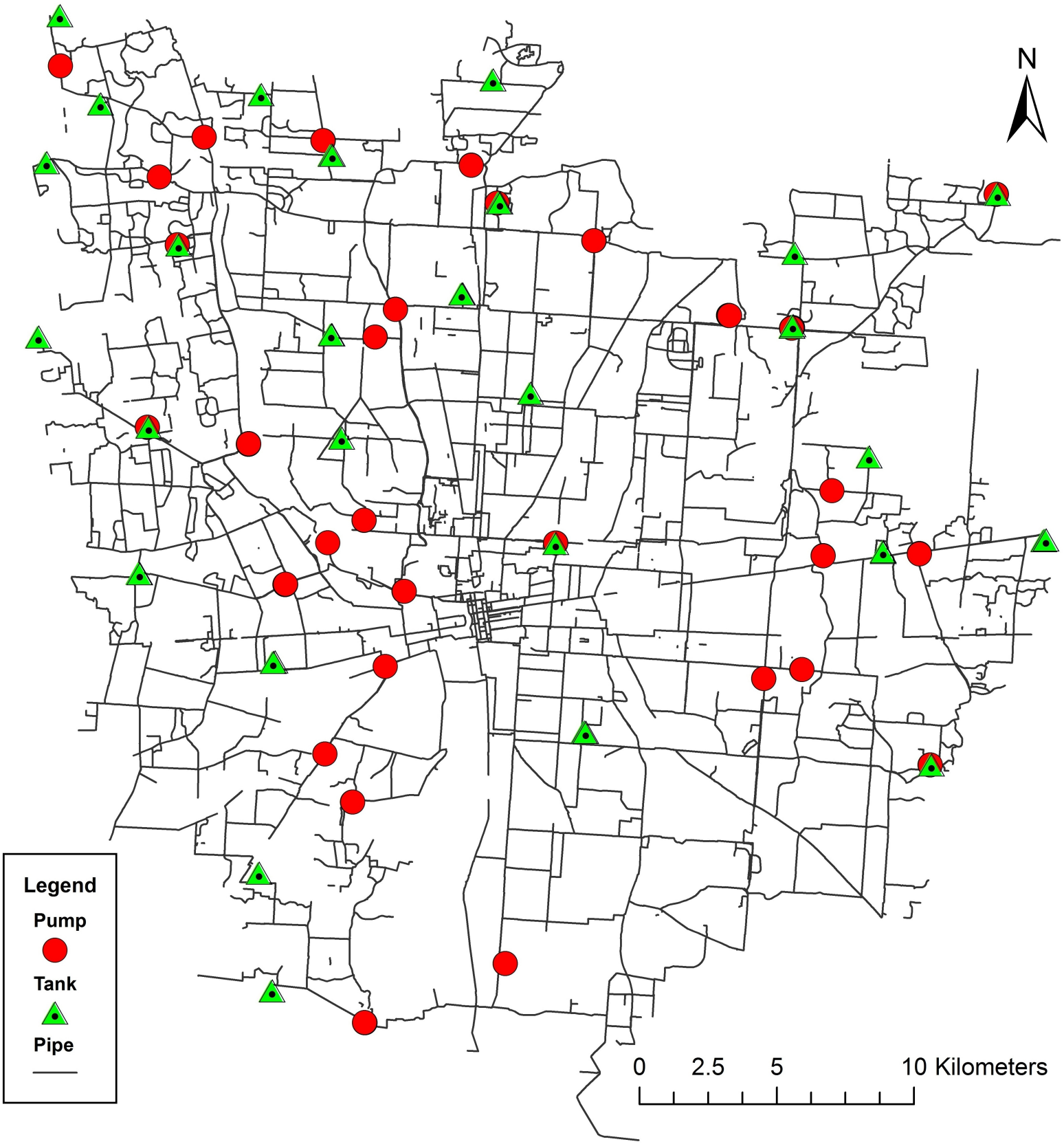

Figure 5

Click here to download Figure Figure 5.pdf

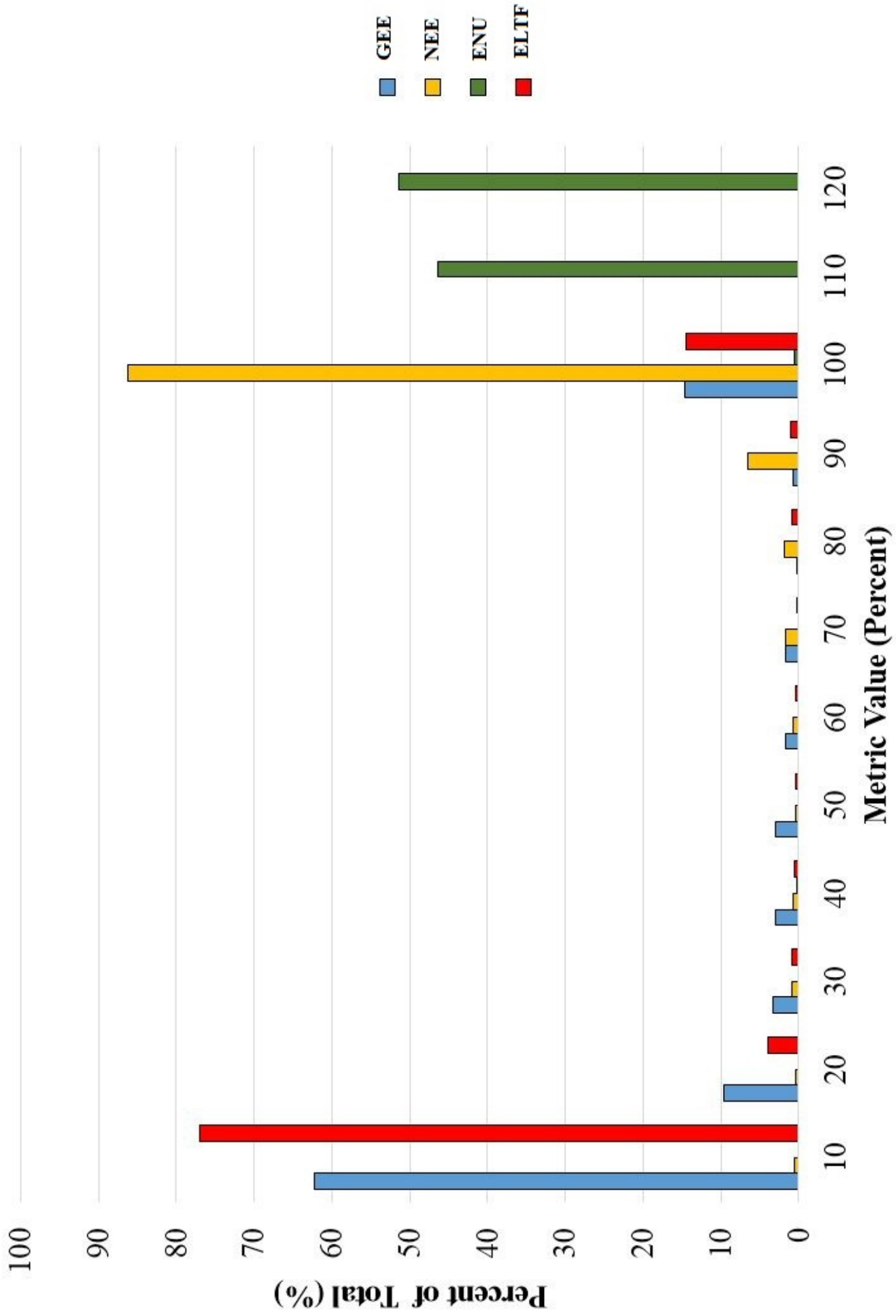

Figure 6a

Click here to download Figure Figure 6a.tif

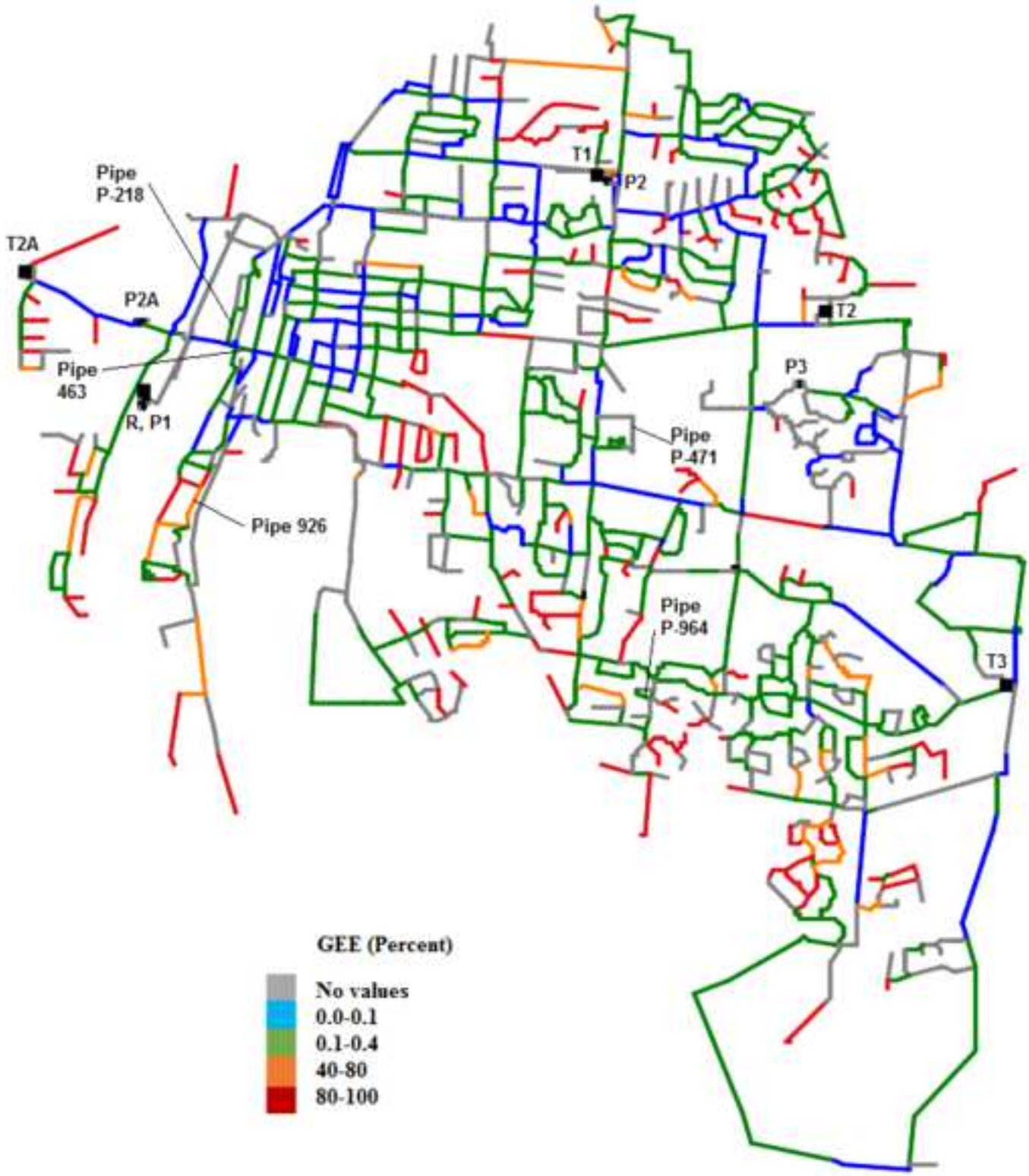

Figure 6b

Click here to download Figure Figure 6b.tif

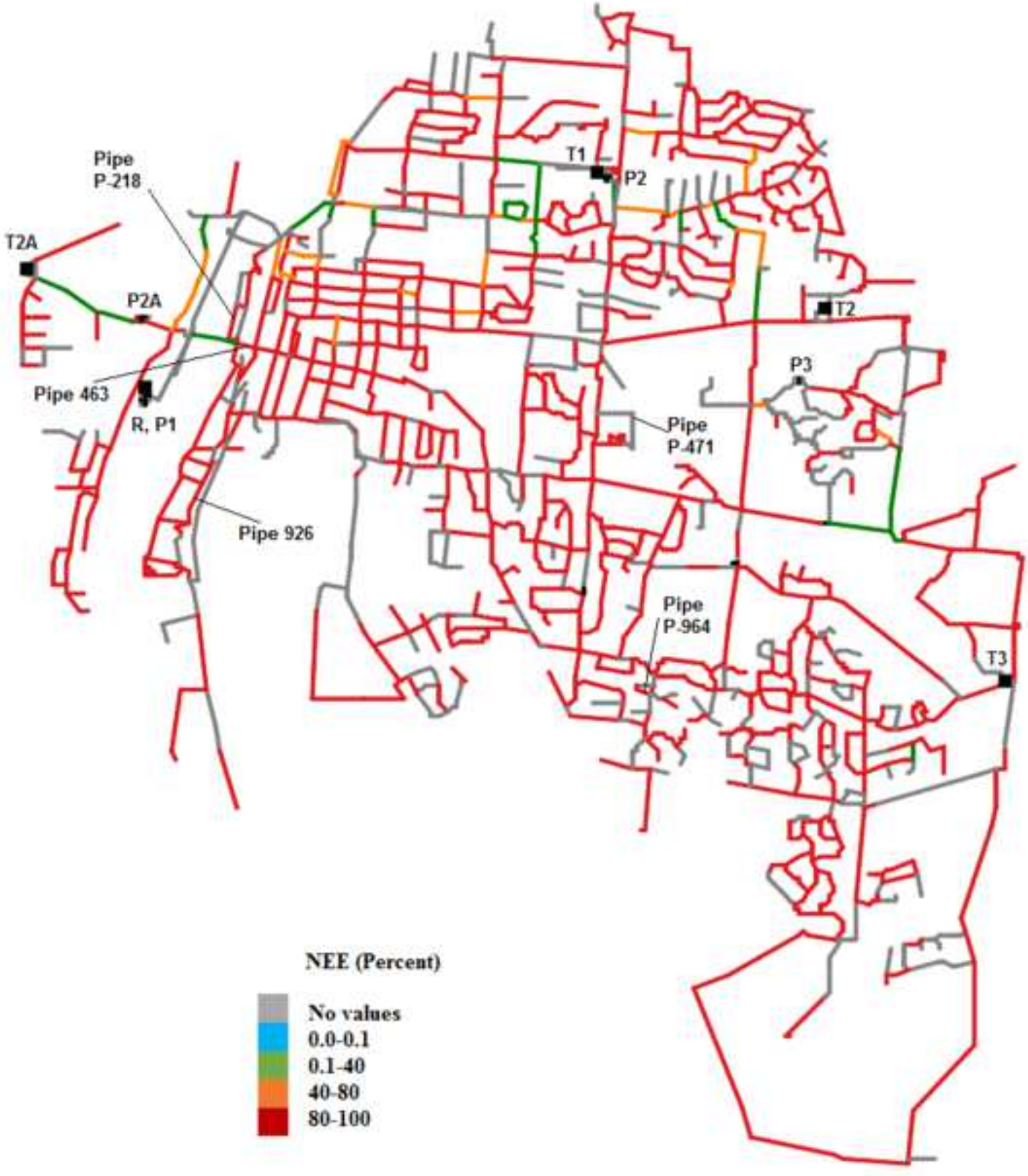

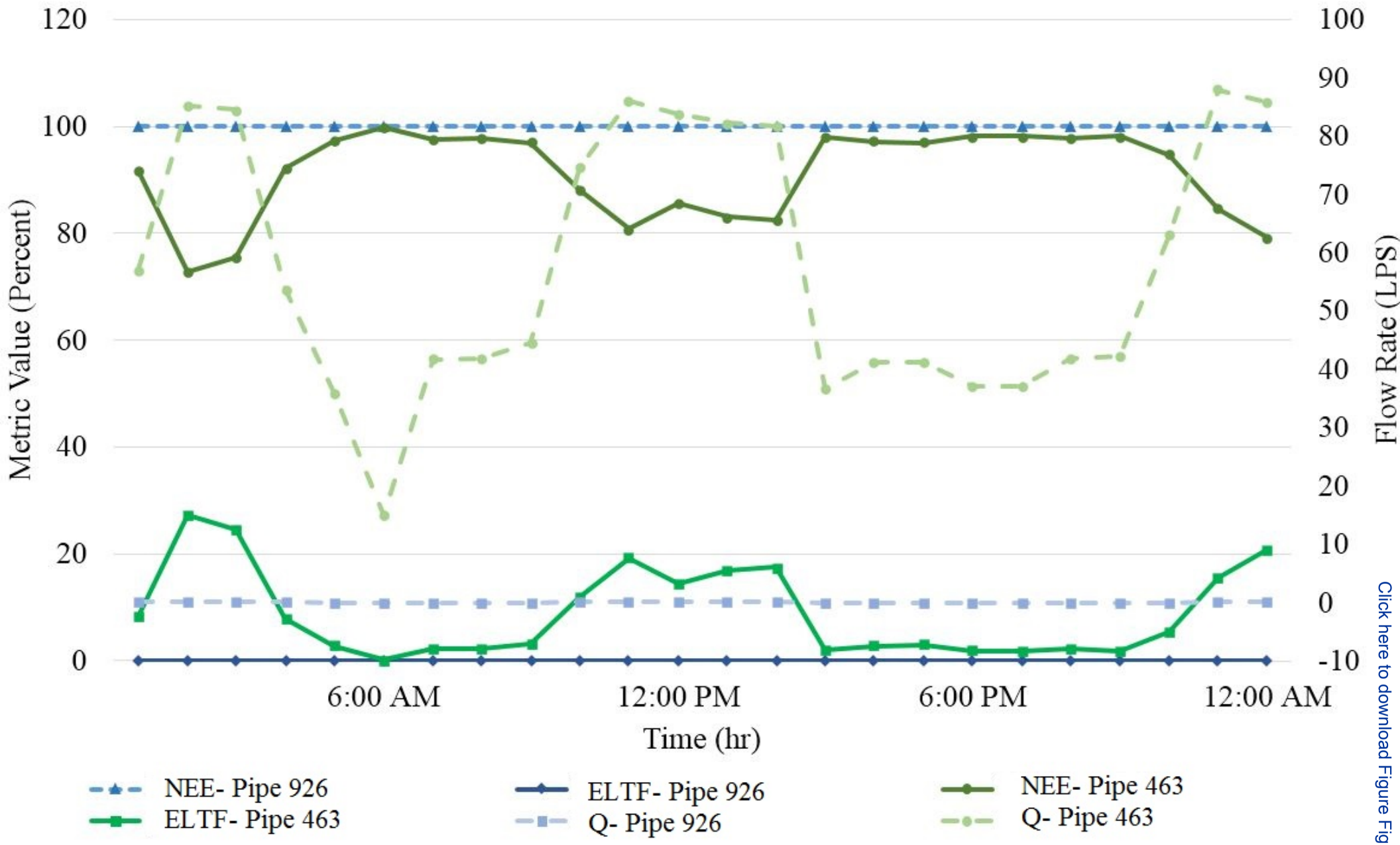

Figure 8

Click here to download Figure Figure 8.pdf

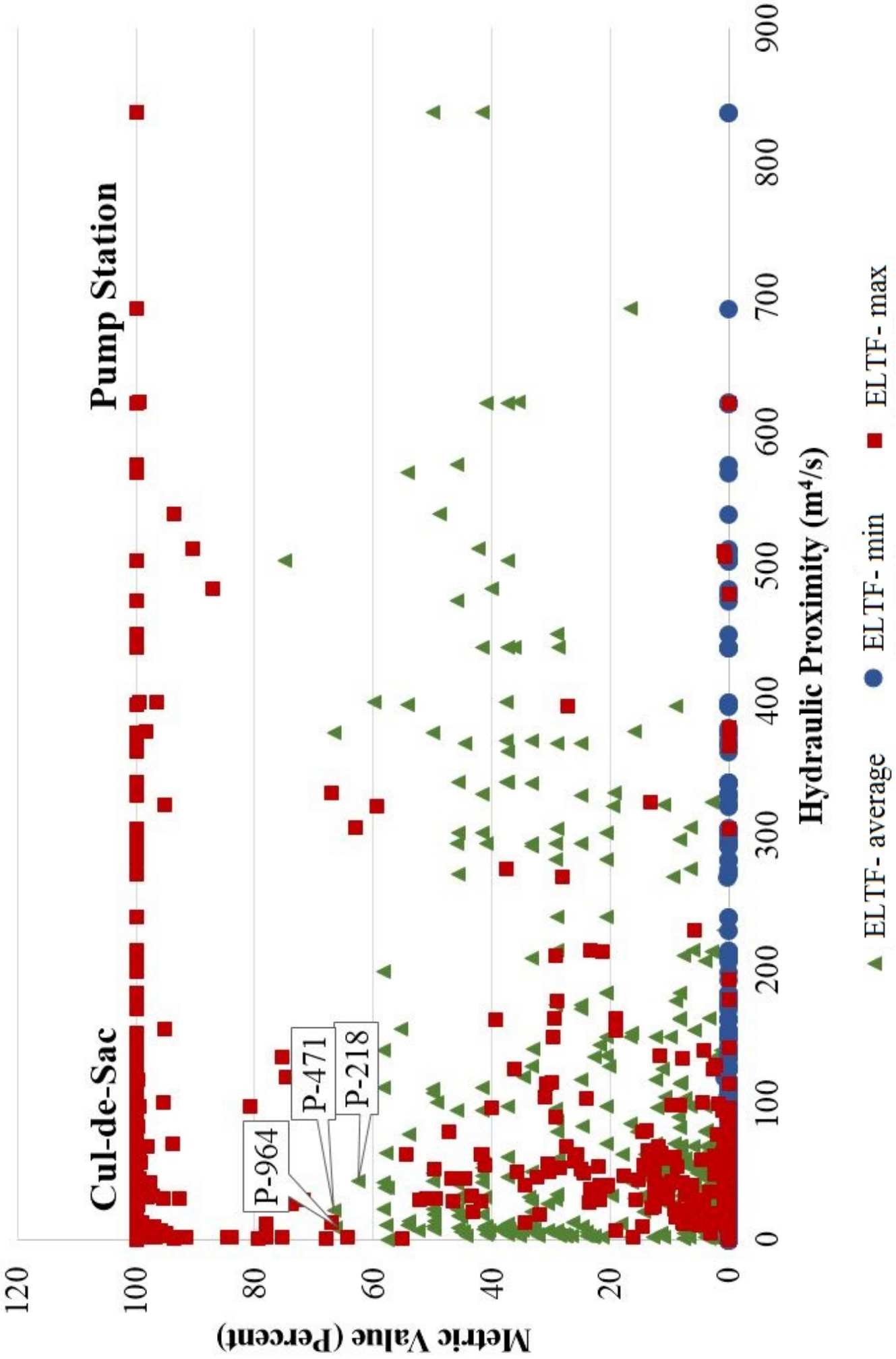

Figure 9

Click here to download Figure Figure 9.pdf

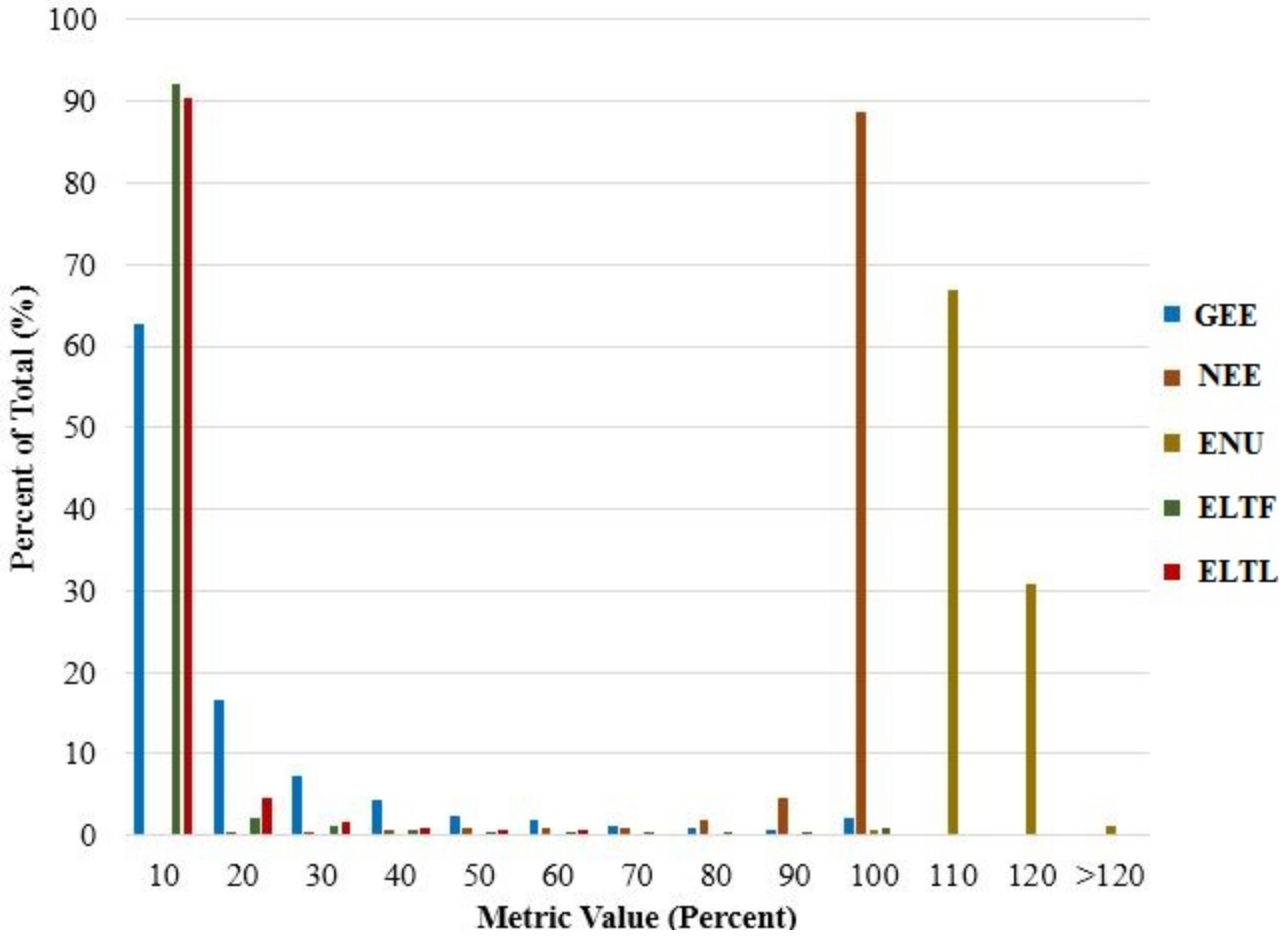

Figure 10

Click here to download Figure Figure 10.pdf

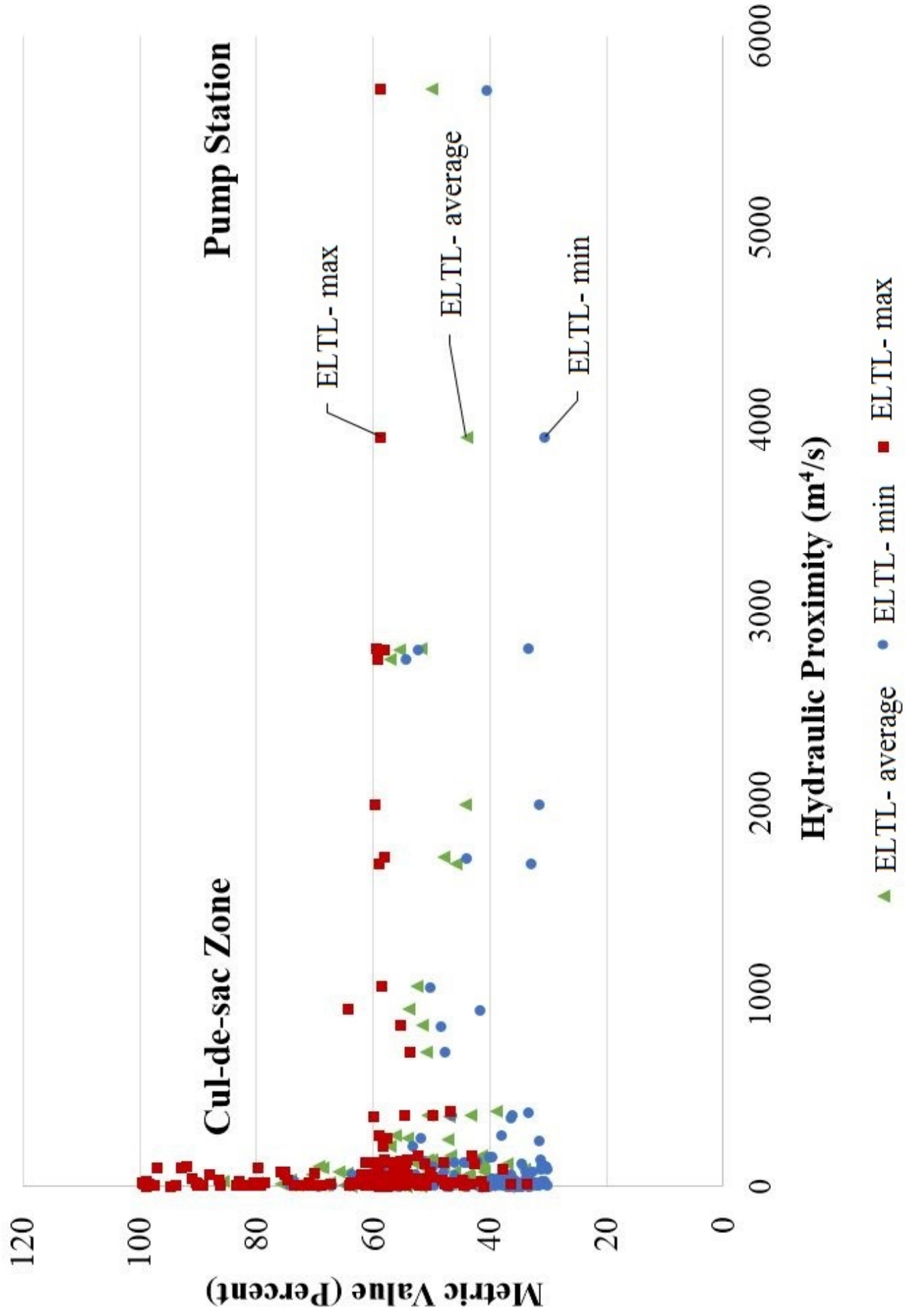

Figure 1. Hydraulic grade line and energy inputs and outputs in a pipe.

Figure 2. a) Example calculation of energy delivered at a model node connected to upstream and downstream pipes; b) model layout of System #1 (reported in Cabrera et al. (2010)) (*L* = pipe length; *D* = pipe diameter; P-10 = pipe ID; J-10 = node/junction ID; *Q* = pipe flow; *El*. = node elevation).

Figure 3. Diurnal demand pattern for Systems #1 through #3 (24-hour period).

Figure 4. a) Model layout of System #2 (medium-sized US Midwest); b) model layout of System #3 (large-sized US Midwest).

Figure 5. Histogram that indicates the percentage of pipes with numerical values of gross energy efficiency (*GEE*), net energy efficiency (*NEE*), energy needed by the users (*ENU*) and energy lost to friction (*ELTF*) in System #2 (medium-sized US Midwest) for the baseline scenario.

Figure 6. a) Numerical values of gross energy efficiency (*GEE*) and (b) net energy efficiency (*NEE*) in pipes of System #2 (medium-sized US Midwest) for the baseline scenario.

Figure 7. Hourly values of net energy efficiency (*NEE*) and energy lost to friction (*ELTF*) in Pipe 463 (near pump station P1) and Pipe 926 (located further away from pump station P1) over the 24-hour diurnal period in System #2 for the baseline scenario. (Flow in Pipes 463 and 926 are also indicated.)

Figure 8. Energy lost to friction (*ELTF*) (as calculated in Eq. 6) and max/min values of energy lost to friction observed over the 24-hour diurnal period (*ELTF*-max, *ELTF*-min) *versus* proximity to a a pump or tank component in System #2 (medium-sized US Midwest) for the baseline scenario.

Figure 9. Histogram that indicates the percentage of pipes with numerical values of gross energy efficiency (*GEE*), net energy efficiency (*NEE*), energy needed by users (*ENU*), energy lost to friction (*ELTF*), and energy lost to leakage (*ELTL*) in System #3 (large-sized US Midwest) for the baseline scenario.

Figure 10. Energy lost to leakage (*ELTL*) (as calculated in Eq. 7) and max/min values of energy lost to leakage observed over the 24-hour diurnal period (*ELTL*-max, *ELTL*-min) *versus* proximity to a pump or tank in System #3 (large-sized US Midwest) for the baseline scenario.